



An aqueous platinum nanotube based fluorescent immuno-assay for porcine reproductive and respiratory syndrome virus detection



Lu Chen^a, Shiyi Ye^a, Kai Cai^a, Cuiling Zhang^b, Guohua Zhou^b, Zhike He^b, Heyou Han^{a,*}

^a State Key Laboratory of Agricultural Microbiology, College of Science, Huazhong Agricultural University, Wuhan 430070, PR China

^b Key Laboratory of Analytical Chemistry for Biology and Medicine (Ministry of Education), College of Chemistry and Molecular Sciences, Wuhan University, Wuhan 430072, PR China

ARTICLE INFO

Article history:

Received 30 March 2015

Received in revised form

11 June 2015

Accepted 20 June 2015

Available online 23 June 2015

Keywords:

PRRSV detection

PtNTs

Quantum dot

Fluorescence

ABSTRACT

Porcine reproductive and respiratory syndrome virus (PRRSV) has been a significant pathogen towards global swine industry upon its emergence in the late 1980s and since then has exemplified a rapidly evolving, widely spreading pathogen. It is urgently important to develop a simple, rapid and cost effective method to detect this pathogen when virus outbreaks. In the present work, it was found that virus antibody modified platinum nanotubes (Pt–Ab) could act as a superquencher to CdTe:Zn²⁺ quantum dots (CdTe:Zn²⁺ QDs) fluorescence by Stern–Volmer constants nearly 10⁹ M⁻¹ without any aggregation, the CdTe:Zn²⁺ QDs fluorescence will recover as the Pt–Ab goes away by antibody and antigen interaction when virus was added into the probe solution, releasing CdTe:Zn²⁺ QDs from the surface of Pt–Ab. By the recovery fluorescence intensity, it can realize qualitative and quantitative detection of PRRSV. This method gives a fast response to PRRSV concentration and provides a sensitive detection limit (2.4 ng/mL). Moreover, it can be applied in infected porcine serum samples and obtain satisfied results.

© 2015 Elsevier B.V. All rights reserved.

1. Introduction

Porcine reproductive and respiratory syndrome virus (PRRSV) is a single-stranded positive-sense RNA virus classified within the family Arteriviridae which has caused a significant economic loss to swine industry worldwide during the past several decades [1]. Once infected by PRRSV, the pregnant pig will produce stillbirth, abortion and finally tortured to death. Since the outbreak in America and Canada in 1987, there have been thousands of pigs that are infected and death. However, it is unfortunate that both traditional control strategies and conventional vaccines are insufficient to provide sustainable control of PRRSV, which is because the PRRSV genes are highly variable. Therefore, development of immune method for rapid PRRSV detection is an urgent desire currently. The usual immune methods are enzyme linked immunosorbent assays (ELISA), virus culture and isolation analysis and fluorescent immune antibody indicator based detection, etc [2,3]. However, these methods require sophisticated performers and tedious steps. Furthermore, these methods cannot provide a fast response to virus concentration and give a precise quantitative result of virus concentration; up to now the fastest semi-quantitative PRRSV detection method requires at least 3 h. Therefore it

urgently needs simple, rapid and cost effective method for PRRSV detection. Fortunately, the emerging of nanotechnology has provided a good solution for quantitative virus detection.

Platinum nanomaterials, including platinum nanoparticles, platinum nanowires, platinum nanospheres, platinum nanotubes have received great attention by chemists over the past few decades due to their extinguished properties, such as good electronic conductivity, favorable biocompatibility, chemical stability, especially intrinsic peroxidase like activity and good binding affinity to amine-containing molecules [4–6]. Among those platinum nanostructures, platinum nanotubes (PtNTs) are specially favored and widely studied because of their unique properties, such as the enhanced catalysis ability, resistance to aggregation, good electrochemistry activity and reduced density [7]. Those superior properties have endowed PtNTs with great diversity in surface functionalization and general application in many fields including electrochemistry, fuel cells, catalysis chemistry and as well as biosensors [8–11].

To the best of our knowledge, many nanomaterial, such as gold nanoparticles, graphene oxide, Fe₃O₄ nanoparticles and carbon nanotube, can be used as fluorescent quenchers and provide a platform for biomolecules sensing [12–15]. Among them, gold nanoparticles can quench quantum dots fluorescence with high efficiency [16]. However, gold nanoparticles are easily aggregated and lead to color change as well as losing quenching effect. Fortunately, platinum nanotubes can solve the problem and it has

* Corresponding author. Fax: +86 27 8728 2043.

E-mail address: hyhan@mail.hzau.edu.cn (H. Han).

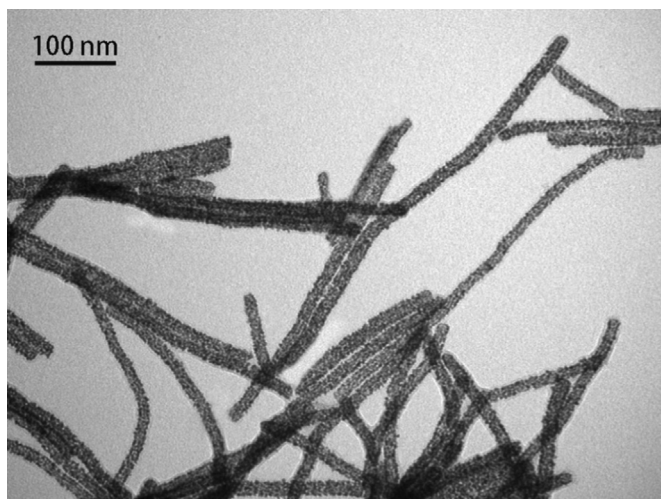
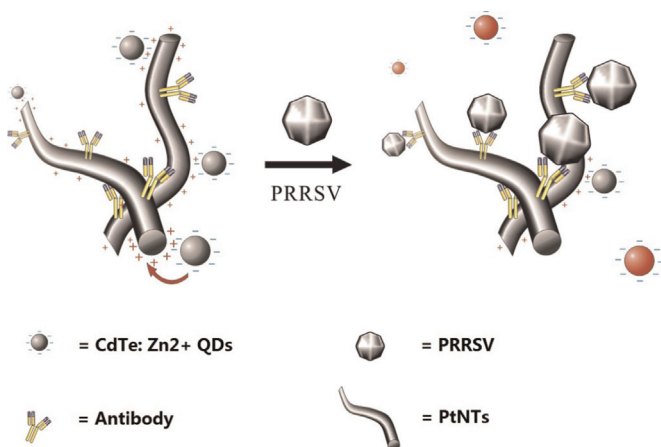


Fig. 1. TEM of platinum nanotubes.



Scheme 1. CdTe:Zn²⁺ QDs and Pt–Ab based fluorescence biosensor for PRRSV detection.

never been reported that platinum nanotubes could act as a good fluorescence quencher towards quantum dots without any aggregation. Herein, it is found that platinum nanotubes shown excellent fluorescence quenching ability towards CdTe: Zn²⁺ QDs fluorescence, with the Stern–Volmer constant nearly 10^9 M^{-1} . As a proof of concept, CdTe:Zn²⁺ QDs were chosen as a fluorophore because they were much lower toxic than CdSe QDs or CdTe QDs reported by our previous synthesis method [17]. The platinum nanotubes, as presented in Fig. 1, were also synthesized according to our group previous work and systematical synthesis and characterization description can be found in this work [18]. Now the CdTe:Zn²⁺ QDs and PtNTs will be employed to design a biosensor for PRRSV detection (Scheme 1) as it is a very harmful pathogen towards global swine industry [19–21].

2. Materials and methods

2.1. Materials

N-acetylcysteine (NAC), Hexadecyltrimethylammonium bromide (CTAB, 99%) was commercially available from Sigma Chemical Co. (St. Louis, MO, USA). Tellurium (reagent powder), CdCl₂ 2.5H₂O, ZnCl₂, and sodium borohydride (NaBH₄) were obtained from Sinopharm Chemical Reagent and were used as capping agents without additional purification. Tellurium dioxide powder

(TeO₂, 99.99%) was purchased from Aladdin Chemistry Co., Ltd. The Pseudorabies MoAb Ascites fluid IgG2b isotype (Ab1, 1 mg/mL) was phased from Veterinary Medical Research & Development (USA). All solutions were prepared using Milli-Q water (Millipore) as the solvent.

2.2. Instruments

Fluorescence measurements were performed on a Shimadzu RF-5301 PC12 spectrofluorophotometer (Shimadzu Co., Kyoto, Japan), and a 0.6 cm path-length quartz cuvette was used in all experiments. UV–vis absorption spectra were recorded on Shimadzu UV-2550 spectrophotometer with baseline corrected. Fluorescence lifetimes were recorded on FLS920 spectrometer using the time correlated single-photon counting (TCSPC) option and the Edinburgh Instruments picoseconds pulsed diode laser (Model: EPL-375) as the light source.

2.3. Preparation of CdTe:Zn²⁺ QDs

In a typical synthesis, sodium borohydride (20 mg) was reacted with tellurium powder (25 mg) in deionized water (1.0 mL) to produce sodiumhydrogen tellurium (NaHTe). The mixture of Zn²⁺-NAC and Cd²⁺-NAC was prepared by dissolving CdCl₂ 2.5H₂O, ZnCl₂, and N-acetyl Cysteine (NAC) in deionized water and adjusting the pH to 9.0 by dropwise addition of NaOH solution (1 M). The fresh NaHTe solution (0.4 mL) was then injected into a N₂-saturated mixture of Zn²⁺-NAC and Cd²⁺-NAC precursor solution under vigorous stirring. The typical molar ratio of Cd, Zn, Te, and NAC introduced was 1:2:0.2:3.6 in a total volume of 40 mL with 6.25 mM of Cd²⁺ concentration. A volume of 40 mL of precursor was put into a teflon-lined stainless steel autoclave with a volume of 50 mL. The autoclaves were maintained at the desired growth temperature (200 °C). Each autoclave was cooled to room temperature at regular time intervals after the initial heating. To remove NAC–Cd/Zn complex at the end of the synthesis, cold 2-propanol was added into the reaction mixture to precipitate NAC-capped CdTe:Zn²⁺ QDs. The as-prepared products were dried overnight under vacuum at 40 °C for further experiments.

2.4. Synthesis of porous Pt nanotubes (PtNTs)

First, TeNWs were prepared according to the method reported by Chang et al. [22]. Typically, Hydrazine monohydrate (5 mL) was added slowly to a beaker containing tellurium dioxide (0.032 g) at room temperature under constant magnetic stirring. After 50 min, the mixture was diluted 10-fold with SDS (10 mM) and then subjected to a centrifugation/wash cycle. Second, TeNWs were used as templates to synthesize PtNTs. In a typical synthesis, TeNWs (~0.01 mmol) were dispersed in 10 mL of CTAB solution (1 mM) under constant magnetic stirring. After 15 min, 0.1 M NaOH was added to the H₂PtCl₆ (~0.002 mmol) to adjust the pH to 7.0, and then the mixture was added to the solution. After 50 min, the mixture was subjected to a centrifugation/wash cycle to remove most of the matrices, including CTAB. Then the flocculation, that was the intermediate products, was re-dispersed in water (0.5 mL) and maintained at room temperature for 3 h. After a centrifugation/wash cycle, porous PtNTs were obtained.

2.5. Preparation and determination of the Pt–Ab conjugation

The as prepared platinum nanotubes were quantitatively determined by direct reading inductively coupled plasma spectrometer and were dissolved in 1.0 mL distilled water. Afterwards, 1 μg PRRSV antibody was added into the solution and mixed well. The Pt–Ab was prepared by physically absorbed of antibody onto

the surface of platinum nanotubes under 277.15 K for 24 h. Afterwards, the Pt–Ab was purified by ultra filtration with 50 K ultra filtration tube. Rotation at 8000 g for 15 min and reverse ultra filtration at 2000 g for 5 min. This step was repeated for at least three times. Finally, the purified Pt–Ab was determined by direct reading inductively coupled plasma spectrometer again. The Pt–Ab concentration was determined by Pt atom concentration. The prepared Pt–Ab was kept in distilled water and restored in refrigerator at 277.15 K until use and can be kept for at least two months without deterioration.

2.6. Virus purification and serum samples collection

For virus propagation, Marc-145 cells with confluence of 70–80% were washed thrice with serum free Dulbecco's modification of Eagle's medium (DMEM, Gibco, USA), and then incubated with PRRSV strain WUH3 (GenBank: HM853637) at 37 °C for 1 h. Afterwards, the infected cells were maintained in DMEM supplemented with 5% fetal bovine serum. Cells were collected after 48 h post infection, freezing-thawing at –80 °C for 3 times. The culture medium was centrifuged at 3000 rpm for 30 min to remove the cell debris. The supernatant was loaded to the ultracentrifuge tube (Beckman) and centrifuged at 26,000 rpm for 2 h at 4 °C. The virus was resuspended with PBS and stored at –80 °C. PRRSV RNA was extracted and reversed transcribed into cDNA using PrimeScript™ RT Master Mix (TaKaRa). PRRSV ORF5 gene was amplified by PCR with the following primers: 5'-GTGGAATTCATGTGGGGAAGTGCT-3' and 5'-GTGAAGCTTCTAGAGACCCCAT-3'. The PRRSV infected pig's vena cava blood was collected by sterile syringes. The collected blood was placed at 37 °C for 1 h, and then put into the refrigerator at 4 °C overnight to precipitate serum. Finally, the samples were purified by ultrafiltration at 3000 rpm for 5 min before use. When performing PRRSV detection experiment, the serum samples were added into the detection buffer solutions.

2.7. Fluorescence measurement

In a typical PRRSV fluorescence detection procedure, first of all, 50 nM CdTe: Zn²⁺ QDs and 4.2 μM Pt–Ab (based on Pt atom concentration) were mixed well. After that, different concentrations of PRRSV were added into the 0.01 mol/L PBS buffer solution (pH7.4) to form a 600 μL detection sample and then recorded the fluorescence spectra. The excitation wavelength was 388 nm and maximum emission wavelength was 613 nm. The excitation and emission slits were both 10 nm. All of the fluorescence measurements were performed under the RF5301 Shimadzu spectrometer at ambient conditions. The serum samples detection was performed under the same steps with only one difference that 10 μL serum was added into the buffer solution before volume was set at 600 μL by 0.01 mol/L PBS solutions.

3. Results and discussion

3.1. Superquenching QDs fluorescence by Pt–Ab

In this work, PRRSV antibody was first adsorbed onto the surface of PtNTs to formed Pt–Ab which acts as both the fluorescence quencher and PRRSV capture probe. The fluorescence quenching intensity was measured by fluorescence spectra. The maximum emission intensity of CdTe:Zn²⁺ QDs is at 613 nm when excited by 388 nm ultraviolet source. Upon addition of different concentrations of Pt–Ab, the fluorescence intensity of CdTe:Zn²⁺ QDs is decreased accordingly. Stern–Volmer relationship is applied to describe the fluorescence intensity variation along with the Pt–Ab concentrations.

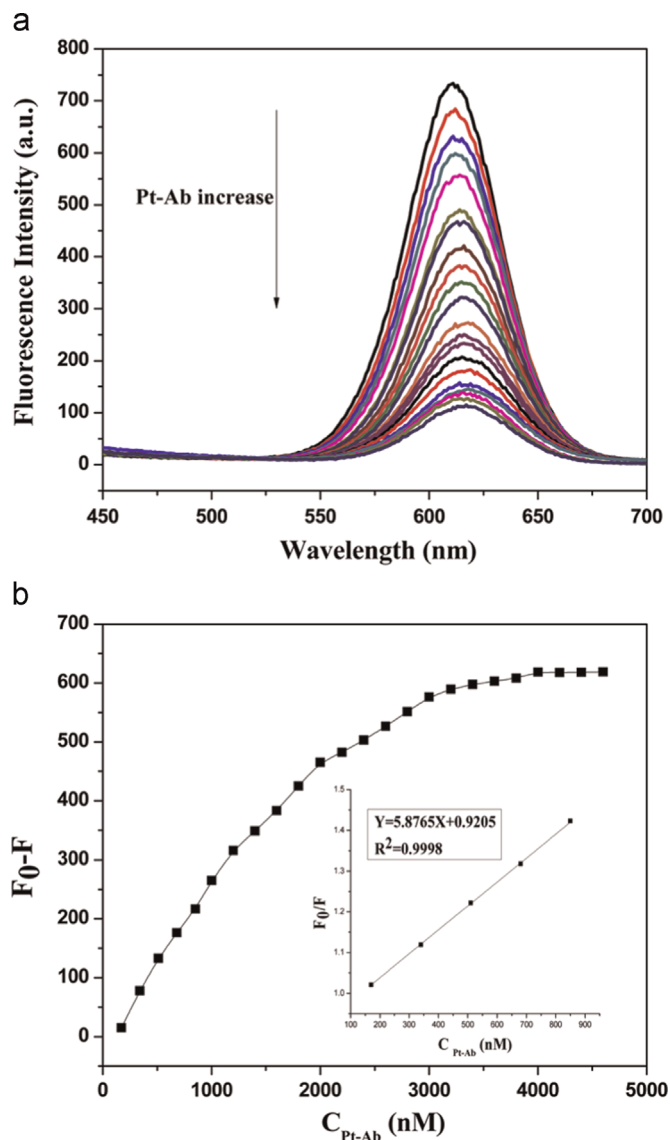


Fig. 2. (a) Fluorescence spectra of 50 nM CdTe:Zn²⁺ QDs quenched by different concentrations of Pt–Ab. (b) Superquenching fluorescence intensity of 50 nM CdTe: Zn²⁺ QDs by 170, 340, 510, 680, 850, 1000, 1200, 1400, 1600, 1800, 2000, 2200, 2400, 2600, 2800, 3000, 3200, 3400, 3600, 3800, 4000, 4200 nM of Pt–Ab. (Inset: The linear relationship between fluorescence quenching intensity and Pt–Ab concentrations.).

$I_0/I = 1 + K_{SV}[Pt-Ab]$ Where I_0 and I are the fluorescence intensities of CdTe:Zn²⁺ QDs in the absence and presence of Pt–Ab, respectively; $[Pt-Ab]$ is the concentration of Pt–Ab; K_{SV} is the Stern–Volmer quenching constant. The relationship between I_0/I and the concentration of Pt–Ab demonstrates the highly efficient quenching produced by Pt–Ab (Fig. 2). As shown in Fig. 2 inset, there is a good linear relationship when the concentration of Pt–Ab is between 170 and 850 nM, and the K_{SV} of Pt–Ab is $5.87 \times 10^9 \text{ M}^{-1}$, which is comparable to the “superquenching” capability of gold nanoparticles towards QDs. Previous studies have proved that the superquenching ability by gold nanoparticles is dynamic quenching [23]. However, there are few reports about the platinum nanotubes quenching mechanism. To clarify the quenching mechanism of Pt–Ab, UV–vis spectra and fluorescence lifetimes were both recorded to demonstrate this issue. As shown in Figs. S1 and S2, the UV–vis spectra of both CdTe:Zn²⁺ QDs and the complex of CdTe:Zn²⁺ QDs and Pt–Ab are almost the same. Moreover the fluorescence lifetimes of CdTe:Zn²⁺ QDs and the

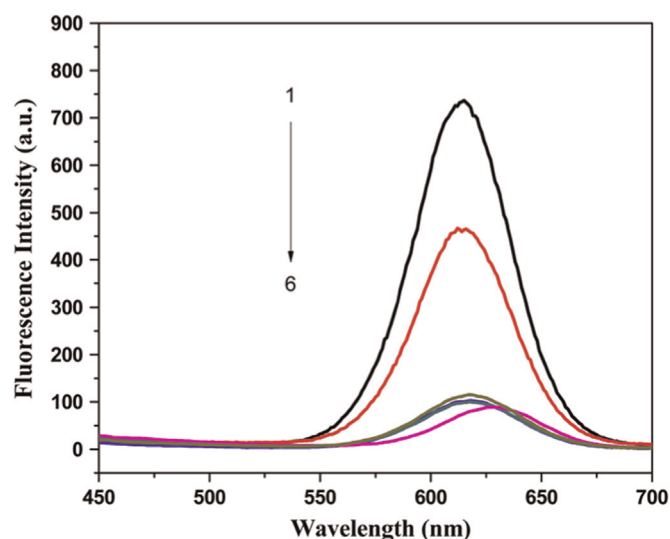


Fig. 3. Fluorescence spectra of CdTe:Zn²⁺ QDs (1); PRRSV induced QDs fluorescence recovery spectroscopy (2); fluorescence spectra of CdTe:Zn²⁺ QDs, Pt-Ab and pseudo rabies virus (3); fluorescence spectra of CdTe:Zn²⁺ QDs, Pt-Ab and swine flu virus (4); fluorescence spectra of CdTe:Zn²⁺ QDs, Pt-Ab (5); fluorescence spectra of CdTe:Zn²⁺ QDs, Pt-Ab and polio virus (6).

complex of CdTe:Zn²⁺ QDs and Pt-Ab are 33 s and 18 s respectively, which are calculated from fluorescence lifetime determination software. Based on these observations, it can be speculated that the quenching mechanism is dynamic mode [24,25]. Then the quenching experiments were conducted at different temperatures, as shown in Fig. S3, the linear relationship between I_0/I and the Pt-Ab are with different slopes, the K_{sv} for Pt-Ab at 293.15 K, 298.15 K and 308.15 K are $5.81 \times 10^9 \text{ M}^{-1}$, $5.87 \times 10^9 \text{ M}^{-1}$ and $5.97 \times 10^9 \text{ M}^{-1}$, respectively. It is clear that the K_{sv} is increased along with the rising temperatures. In a conclusion, it strongly confirms that the CdTe:Zn²⁺ QDs fluorescence quenching mechanism by platinum nanotubes is dynamic quenching [26]. We reason that the superquenching ability by Pt-Ab towards CdTe:Zn²⁺ QDs fluorescence can be used as a good fluorescent probe. Therefore, it is adopted in a homogenous PRRSV detection. In order to utilize the superquenching ability by Pt-Ab towards CdTe:Zn²⁺ QDs fluorescence, a homogenous virus detection method is designed as follows: first, Pt-Ab strongly quenches the fluorescence of CdTe:Zn²⁺ QDs and they are composed of a virus capture probe, then PRRSV is added into the probe solution, the fluorescence of CdTe:Zn²⁺ QDs is recovered by immune interaction between Pt-Ab and PRRSV. The PRRSV induced release of CdTe:Zn²⁺ quantum dots from the surface of Pt nanotubes may due to the steric hindrance by virus-antibody complex which effectively prevents CdTe:Zn²⁺ quantum dots to interact with Pt nanotubes. By the recovery fluorescence intensity, it can be quantitatively determined the PRRSV concentration rapidly.

3.2. Feasibility of the virus biosensor

To clarify the fluorescence recovery is due to the interaction between antibody and PRRSV. First of all, PRRSV and its antibody were added respectively into the CdTe:Zn²⁺ QDs solution to investigate the fluorescence intensity variation. Fig. S4 has shown that both virus and its antibody cannot quench or greatly enhance the fluorescence intensity of CdTe:Zn²⁺ QDs. So the fluorescence quenching is caused by PtNTs and the fluorescence recovery is due to the immune interaction between Pt-Ab and its target virus PRRSV which may partially put the CdTe:Zn²⁺ QDs distant away from the surface of Pt-Ab. This detection strategy has provided a rapid and sensitive homogenous virus detection method.

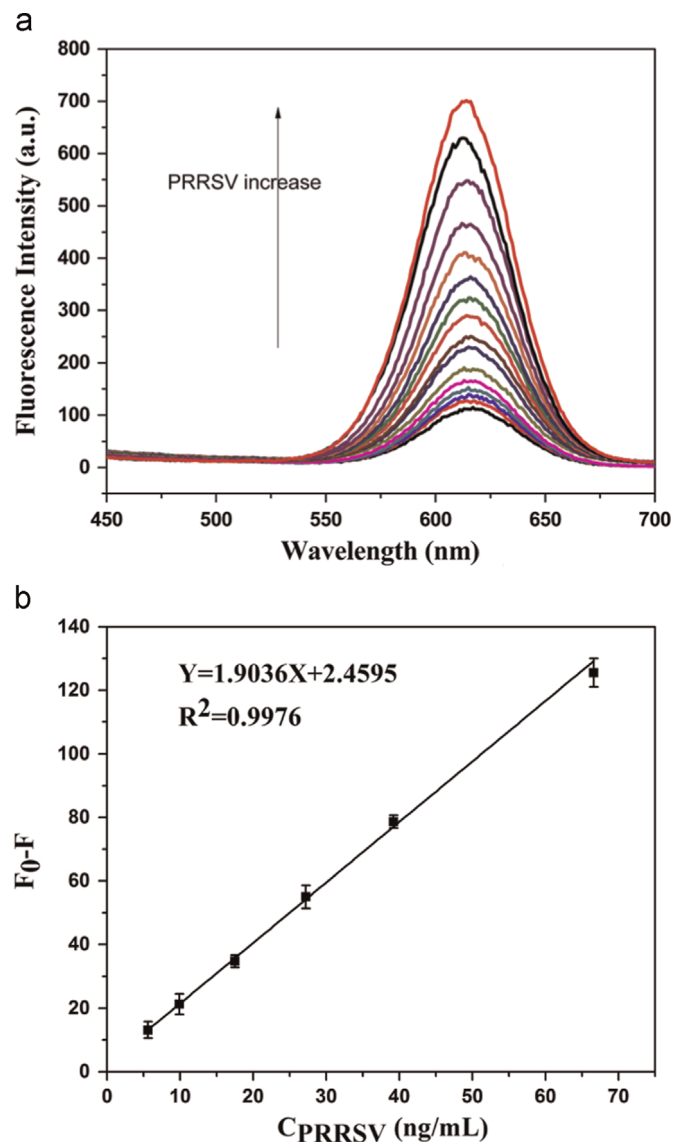


Fig. 4. (a) Fluorescence spectra of 50 nM CdTe:Zn²⁺ QDs, 4.2 μM Pt-Ab and different concentrations of PRRSV in aqueous solution; (b) linear curve of CdTe:Zn²⁺ QDs and Pt-Ab based biosensor for PRRSV detection in aqueous solution.

Table 1
Analysis results for PRRSV detection in clinical samples.

	Added	Founded	Mean recovery	RSD (%) (n=3)
Sample 1	8.00	7.98 ± 0.02	99.7	1.4
	16.00	15.88 ± 0.05	99.2	2.6
	24.00	24.75 ± 0.08	100.1	1.7
Sample 2	8.00	8.25 ± 0.03	100.3	0.8
	16.00	16.38 ± 0.06	100.2	1.3
	24.00	23.96 ± 0.05	99.8	2.5
Sample 3	8.00	8.04 ± 0.06	100.5	0.9
	16.00	15.92 ± 0.04	99.5	1.6
	24.00	24.32 ± 0.02	100.2	2.4

3.3. Specificity of the virus biosensor

The specificity of this biosensor is determined by virus purity and immune recognition between PRRSV and its antibody. The PRRSV was purified by centrifugation protocol and the result is shown in Fig. S5 [27]. From the purified virus result by electrophoresis, it can be seen that the PRRSV is very pure. To investigate

the selectivity of this method, three other kinds of viruses are chosen as a control. Fig. 3 has shown that the PRRSV and its antibody have a good affinity which recovers the fluorescence intensity of CdTe:Zn²⁺ QDs easily, whereas other viruses cannot recover the fluorescence intensity of CdTe:Zn²⁺ QDs obviously.

3.4. Sensitivity of this virus biosensor

The sensitivity of this proposed superquenching system for PRRSV assay is investigated by analyzing different concentrations of target virus under the same experimental condition. Fig. 4 (a) depicts the fluorescence spectra of the biosensor upon analyzing PRRSV with different concentrations. As the concentration of PRRSV increases, the fluorescence of CdTe:Zn²⁺ QDs recovers accordingly. Fig. 4(b) depicts the calibration curve corresponding to the recovery fluorescence intensity increase of CdTe:Zn²⁺ QDs upon analyzing PRRSV concentration from 5.6 ng/mL to 66.6 ng/mL. The calibration curves show an excellent linearity with a correlation coefficient of 0.9965. Based on 3σ ($\sigma = S_0/S$; S_0 , standard deviation of blank sample; S , the slope of the calibration curve), the detection limit for PRRSV is estimated to be 2.4 ng/mL.

3.5. Spiking serum samples analysis

To demonstrate this homogenous PRRSV detection method could be applied in clinical analysis, three infected pigs' serum samples were collected and analyzed by 8.00 to 24.00 ng/mL PRRSV spiking serum samples, as shown in the Table 1. The founded virus concentration turns out to be consistent with the added concentration with the quantitative recovery from 98.2% to 100.5%, which demonstrated this CdTe:Zn²⁺ QDs and Pt–Ab based method could apply to clinical sample analysis.

4. Conclusion

In summary, a homogenous assay for PRRSV detection is developed based on aqueous and porous platinum nanotubes super quenching ability towards the fluorescence of CdTe:Zn²⁺ QDs. By modifying the surface of porous platinum nanotubes with virus antibody, it can quench CdTe:Zn²⁺ QDs fluorescence with high efficiency. Meanwhile, the composite acts as a good fluorescence probe for capturing PRRSV in aqueous solution. Due to the unique properties including good biocompatibility, aqueous solubility as well as the excellent fluorescence quenching capacity, porous platinum nanotubes have shown great potentials in biosensor development. It is believable that the porous platinum nanotubes will show more excellent properties in other biosensor applications.

Acknowledgment

This work was financially supported by the National Natural Science Foundation of China (21175051, 21305049). The work is also supported by the Fundamental Research Funds for the Central China Universities (52902-0900206173).

Appendix A. Supplementary material

Supplementary data associated with this article can be found in the online version at <http://dx.doi.org/10.1016/j.talanta.2015.06.061>.

References

- [1] K.K. Conzelmann, N. Visser, W.P. Van, *Virology* 193 (1997) 329–339.
- [2] Y.B. Jiang, S.B. Xiao, L.R. Fang, *Vaccine* 24 (2006) 2869–2879.
- [3] S.M. Lee, S.B. Kleiboeker, *Virology* 342 (2005) 47–59.
- [4] H.M. Zheng, R.K. Smith, Y.W. Jun, C. Kisielowski, U. Dahmen, *Science* 324 (2009) 1309–1312.
- [5] A. Elder, H. Yang, R. Gwiazda, X.W. Teng, S. Thurston, H. He, G. Oberdoster, *Adv. Mater.* 19 (2007) 3124–3129.
- [6] M.N. Nadagouda, R.S. Varma, *Green Chem.* 8 (2006) 516–518.
- [7] H. Wang, S. Li, Y.M. Si, *Nanoscale* 6 (2014) 8107–8116.
- [8] A. Sun, Q.G. Qi, X.N. Wang, P. Bie, *Biosens. Bioelectron.* 57 (2014) 16–21.
- [9] W.J. Xu, Y.M. Wu, H.Y. Yi, L.J. Bai, Y.Q. Chai, R. Yuan, *Chem. Commun.* 50 (2014) 1451–1453.
- [10] H.H. Gong, S.B. Hong, S.C. Hong, *Macromol. Res.* 22 (2014) 397–404.
- [11] G.X. Zhang, S.H. Sun, M. Cai, Y. Zhang, R.Y. Li, X.L. Sun, *Sci. Rep.* 3 (2013) 1526–1534.
- [12] C.H. Lu, H.H. Y, C.L. Zhu, X. Chen, G.N. Chen, *Angew. Chem. Int. Ed.* 48 (2009) 4785–4787.
- [13] C.J. Yu, S.M. Wu, W.L. Tseng, *Anal. Chem.* 85 (2013) 8559–8565.
- [14] R.H. Yang, J.Y. Jin, Y. Chen, N. Shao, H.Z. Kang, Z.Y. Xiao, Z.W. Tang, Y.R. Wu, Z. Zhu, W.H. Tan, *J. Am. Chem. Soc.* 130 (2008) 8351–8358.
- [15] E. Dulkeith, M. Ringle, T.A. Klar, J. Feldmann, *Nano Lett.* 5 (2005) 585–589.
- [16] Z.H. Sheng, H.Y. Han, D.H. Hu, J.G. Liang, Q.G. He, M.L. Jin, R. Zhou, H.C. Chen, *Chem. Commun.* 1 (2009) 2559–2561.
- [17] D. Zhao, Y. Fang, H.Y. Wang, *J. Mater. Chem.* 21 (2011) 13365–13370.
- [18] K. Cai, Z.C. Lv, K. Chen, L. Huang, J. Wang, F. Shao, Y.J. Wang, H.Y. Han, *Chem. Commun.* 49 (2013) 6024.
- [19] I. Trus, C. Bonckaert, K. Meulen, H.J. Nauwynck, *Vaccine* 32 (2014) 2996–3003.
- [20] L.K. Kvisgaard, C.K. Hjulsgaard, C.S. Kristensen, K.T. Lauritsen, L.E. Larsen, *Virus Res.* 178 (2013) 197–205.
- [21] S.H. Yin, C.T. Xiao, P.F. Gerber, N.M. Beach, X.J. Meng, P.G. Halbur, T. Opriessing, *Virus Res.* 178 (2013) 445–451.
- [22] Z.H. Lin, Z. Yang, H.T. Chang, *Cryst. Growth Des.* 8 (2008) 351–357.
- [23] S. Maylio, M.A. Closter, M. Wunderlich, A. Lutich, T.A. Klar, A. Nichtl, K. Kurzinger, F.D. Stefani, J. Feldmann, *Nano Lett.* 9 (2009) 4558–4563.
- [24] M. Oishi, A. Tamura, T. Nakamura, Y. Nagasaki, *Adv. Funct. Mater.* 19 (2009) 827–834.
- [25] Y.Q. Tu, P. Wu, H. Zhang, *Chem. Commun.* 48 (2012) 10718–10720.
- [26] L.M. Ao, F. Gao, B.F. Pan, *Anal. Chem.* 78 (2006) 1104–1106.
- [27] K.K. Conzelmann, N. Visser, P.V. Woensel, H.J. Thiel, *Virology* 193 (1993) 329–339.